Am J Cancer Res 2024;14(12):5644-5664
www.ajcr.us /ISSN:2156-6976/ajcr0159876

Original Article

Cardamonin anticancer effects through the modulation of the tumor immune microenvironment in triple-negative breast cancer cells

Patricia Mendonca[1,2], Sukhmandeep Kaur[1], Bhonesa Kirpal[1], Karam FA Soliman[1]

[1]*Division of Pharmaceutical Sciences, College of Pharmacy and Pharmaceutical Sciences, Institute of Public Health, Florida A&M University, Tallahassee, FL 32307, The United States;* [2]*Department of Biology, College of Science and Technology, Florida A&M University, Tallahassee, FL 32307, The United States*

Received August 17, 2024; Accepted October 21, 2024; Epub December 15, 2024; Published December 30, 2024

Abstract: The tumor immune microenvironment (TIME) plays a critical role in cancer development and response to immunotherapy. Immune checkpoint inhibitors aim to reverse the immunosuppressive effects of the TIME, but their success has been limited. Immunotherapy directed at PD-1/PD-L1 has been widely employed, yielding positive results. Unfortunately, the gradual emergence of resistance to PD-1/PD-L1 inhibition has diminished the effectiveness of this immunotherapy in cancer patients, emphasizing the need for new compounds that will be more effective in managing immunotherapy. This study investigated the effect of the natural compound cardamonin on PD-L1 expression and its ability to modulate the TIME, which could overcome immunotherapy resistance in triple-negative breast cancer (TNBC). This investigation used two genetically distinct triple-negative breast cancer cell lines, MDA-MB-231 (MDA-231) and MDA-MB-468 (MDA-468). The results show that TNBC cell treatment with cardamonin inhibited PD-L1 expression and reduced JAK1 and STAT3 levels in MDA-231 cells, while it increased JAK1 expression in MDA-468 cells. Also, cardamonin increased the expression of Nrf2 in both cell lines. In addition, cardamonin decreased MUC1, NF-κB1, and NF-κB2 expression in MDA-MB-231 cells and selectively reduced NF-κB1 expression in MDA-468 cells. Furthermore, cardamonin very potently reduced the inflammatory cytokine CCL2 levels. The decrease in CCL2 release reduces the chemoattraction of macrophages in the tumor microenvironment, which may increase the effectiveness of PD-1/PD-L1 inhibition and allow T-cell infiltration. These findings suggest that the cardamonin modulation of TIME holds promise in reversing resistance of PD-1/PD-L1 inhibition when it is used along with immunotherapy in TNBC treatment.

Keywords: Cardamonin, TNBC, immune resistance, PD-L1, Nrf2, CCL2, tumor immune microenvironment

Introduction

Breast cancer (BC) remains the most prevalent disease and prominent cause of tumor-associated mortality among women. Meanwhile, Triple-Negative Breast Cancer (TNBC) represents 15-20% of all BCs. TNBC is highly invasive and lacks three common receptors found in other types of BC: estrogen, progesterone, and human epidermal growth factor receptor 2. TNBC is differentiated by a unique molecular profile, aggressive character, distinct metastatic outline, and lack of targeted therapies, which challenges current therapy options [1]. Although chemotherapy remains the backbone of BC treatment, with continuous treatment, the tumors become resistant to the cytotoxic drugs in most TNBC patients, who become unresponsive to the drugs [2], leading to relapses and metastasis to other parts of the body [3].

Since the last decade, cancer treatments have gone through a revolution. Cancer tumors were broadly targeted toward using antibody-based immunotherapies that can modulate immune responses against tumors. The use of "immune-checkpoint blockade" to stop the receptor and/or ligand interactions of molecules, such as the programmed cell death protein 1 (PD-1) and its ligand (PD-L1), which reduce T cell activation or function [4]. This type of therapy has shown substantial clinical benefits to many breast cancer patients [5].

https://doi.org/10.62347/ANXS3815

Moreover, recent advances in immunotherapy have highlighted the need to target the tumor immune microenvironment (TIME) to enhance treatment efficacy [5]. TIME is critical in cancer development and treatment resistance, affecting patients' clinical outcomes [5]. The TIME is composed of tumor and non-tumor cells involving multiple cytokines. Because of the dynamic nature of the TIME, secretion of cytokines, growth factors, and tissue matrix remodeling by tumor cells are involved in the suppression of immune cells [6]. These cells develop complex associations throughout the malignant progression by activating the inhibitory immune checkpoints, causing treatment resistance [5].

In the tumor microenvironment (TME), CCL2/MCP1 (Chemokine C-C Motif Ligand 2/Monocyte Chemotactic Protein-1) is a critical mediator between tumor and host cells. CCL2 is considered the strongest chemoattractant chemokine associated with the recruitment of macrophages and a potent inflammation initiator. It was reported to attract other host cells in the TME and regulate their differentiation in collaboration with other cytokines [7]. The distinct mechanisms used by CCL2 to regulate the tumor immune microenvironment are strictly controlled by tumor and tumor-infiltrating immune cells and the tumor stroma. CCL2 overexpression induces tumor metastasis, invasion, and immune resistance, and in tumor patients, it represents a poor prognosis due to the accumulation of immunosuppressive cell subtypes [7].

Moreover, activating mTOR, the downstream signal of the PI3K/AKT signaling, and NF-κB enhanced the expression and release of CCL2, inducing the recruitment of tumor-associated macrophages (TAMs) [8]. Also, NF-κB activation enhances inflammation via cytokines up-regulation and immune response by activating chemokines, including CCL2 [9]. The blockage of the CCL2 receptor, named CCR2, enhanced the therapeutic efficacy of the PD-1 inhibition in cancers, indicating that the combination of anti-PD-1/PD-L1 and CCR2-targeted therapy may lead to better efficacy when compared to either agent alone [10]. CCL2 inhibits trafficking of cytotoxic T cells by binding with CCR2 of the T cell receptor [11]. Thus, when CCL2 and PD-L1 are induced at the same time by PI3K/AKT and NF-κB activation, PD-1/PD-L1 inhibitor resistance can occur due to the release of CCL2, even though the PD-L1 inhibitor entirely blocks PD-L1 [12].

The PD-1/PD-L1 axis is one of the main pathways of tumor immune escape, suggesting that regulating PD-L1 expression could help to manipulate the TIME components [13]. Hence, blocking immune checkpoints, such as PD-1 and PD-L1, can improve the therapeutic effect against tumors by boosting the activity of cytotoxic T cells in the TIME [12]. On the other hand, Nrf2, an upstream transcriptional activator, can also regulate PD-L1 expression. Nrf2 and PD-L1 signaling were reported to co-regulate cancer functions, which can be considered a prospective alternative strategy for PD-1/PD-L1 antibody-based treatments [14]. Also, NF-κB, an essential key to inflammatory processes and immunity, has emerged as a critical positive regulator of PD-L1 expression [15, 16].

Although studies show that patients who show high levels of PD-L1 expression from tumor cells are more likely to benefit from immune checkpoint inhibitors, PD-L1 expression alone cannot adequately predict the efficacy of these inhibitors [17-19]. Therefore, investigating compounds that can inhibit PD-L1 levels and modulate the components of the TIME is crucial to developing more effective immunotherapies.

A recent approach to developing better therapeutic agents with less toxicity and side effects for treating TNBC and with the potential to overcome drug resistance and immune resistance is the investigation of natural compounds, specifically flavonoids [20, 21]. Multiple articles have described their great potential as anticancer compounds that modulate ROS-scavenging enzyme activities, induce cell cycle arrest and apoptosis, modulate autophagy, suppress proliferation and invasiveness of cancer cells, and modulate signaling pathways that are activated during cancer development and progression [22-25]. Cardamonin is a flavonoid that has been described as a promising anticancer agent against breast [26, 27], cervical [28], colon [29, 30], gastric [31], lung [32, 33], ovarian [34], and prostate cancer [35, 36]. In TNBC cells, cardamonin showed cytotoxicity by inducing apoptosis and cell cycle arrest via modulation of Bcl-2, Bax, cyt-C, cleaved caspase-3, and PARP [27]. It also downregulated invasion and migration of cells and reduced stability and nuclear translocation of β-catenin, accompa-

nied by downregulation of β-catenin target genes [27]. Moreover, cardamonin inhibited MDA-231 and MCF-7 BC cell proliferation by inducing G2/M arrest and apoptosis [26]. Although many studies have described the potential effects of cardamonin against BC, its molecular mechanisms in the modulation of the TNBC TIME are still to be clarified.

This study aimed to investigate the molecular mechanisms of cardamonin in affecting the TIME through inhibition of the immune checkpoint PD-L1 and modulation of NF-κB, Nrf2, CCL2, and other mediators that enhance PD-L1 expression in tumor cells. This study hypothesized that by modulating the expression of Nrf2 and decreasing NF-κB and CCL2 levels, cardamonin would downregulate the expression of PD-L1 and help to overcome drug and immune resistance. The cardamonin effects were investigated in two genetically distinct TNBC cell lines, MDA-MB-231 (MDA-231) and MDA-MB-468 (MDA-468).

Materials and methods

Reagents

Cardamonin purity ≥ 98% (HPLC grade), Alamar Blue®, dimethyl sulfoxide (DMSO), chloroform, Interferon-gamma (IFN-γ), and isopropyl alcohol were purchased from Sigma-Aldrich Co. (St. Louis, MO, USA). Fetal bovine serum heat-inactivated (FBS-HI), Dulbecco's modified Eagle's medium (DMEM) high glucose; penicillin/streptomycin and phosphate-buffered saline (PBS) were purchased from Genesee Scientific (San Diego, CA, USA), and TRIzol from Thermo Fischer Scientific (Wilmington, DE, USA). The SYBR Green, iScript advanced reverse transcriptase kit, and specific primers were purchased from Bio-Rad (Hercules, CA, USA). The Wes analysis plates and reagents were obtained from ProteinSimple (San Jose, CA, USA). Antibodies were purchased from Cell Signaling Technology (Danvers, MA, USA). The ELISA kit for PD-L1 (Cat# ELH-B7H1-1) and CCL2 (Cat# ELH-MCP1) and tumor necrosis factor-alpha (TNF-α) were purchased from RayBiotech (Norcross, GA, USA).

Cell culture

TNBC cell lines MDA-231 (Caucasian American) and MDA-468 (African American) were purchased from the American Type Culture Collection (ATCC). The cells were cultured in DMEM supplemented with 10% FBS-HI and 1% penicillin (100 U/mL)/streptomycin (0.1 mg/mL). Cells were incubated at 5% CO_2 and 37°C, subcultured in T-75 flasks, and left to grow to 90% confluency before starting the experiments. The DMEM experimental medium was supplemented with 2.5% FBS-HI; no penicillin/streptomycin was added.

Cell viability

The TNBC cells were seeded at a density of 3×10^4 cells/100 µL/well in 96-well plates and incubated overnight using experimental media. The next day, cells were treated with DMSO, IFN-γ (100 ng/mL), and cardamonin (concentrations ranging from 0.78-200 µM) with or without IFN-γ (100 ng/mL) and incubated for another 24 h. The cells were treated with IFN-γ 1 h before adding cardamonin concentrations. The compound was dissolved in DMSO, with a final concentration not exceeding 0.1%. Each treatment (volume of 100 µL) was added to the plates containing cells, with a final volume of 200 µL. A volume of 20 µL of Alamar Blue® solution (0.5 mg/mL) (Resazurin) assay was used to assess cell viability and was incubated for 4 h. Then, a microplate reader Infinite M200 (Tecan Trading AG) was used to read the fluorescence of excitation/emission at 550/580 nm wavelengths. Fluorescence changes were observed as resazurin was reduced to resorufin by the viable cells. The fluorescent signal was proportional to the number of viable cells in each treatment, and the data were shown as a percentage of alive, untreated controls.

Real-time polymerase chain reaction (RT-PCR)

RNA isolation: Cells were exposed to treatments for 24 h, including DMSO, cardamon-treated (12-50 µM), TNF-α-stimulated (50 ng/mL) or IFN-γ-stimulated (100 ng/mL), and co-treated with cardamonin + TNF-α (50 ng/mL) or IFN-γ (100 ng/mL), according to the purpose of each experiment. The cells were treated with IFN-γ or TNF-α 1 h before adding cardamonin concentrations. After 24 h, cells were harvested, and cell pellets were prepared. Each pellet was homogenized with 1 mL of TRIzol, and 200 µL of chloroform was added to each lysed sample. For 3-5 min, the samples were sat on a rack at room temperature, vortexed for 15-30 sec, and then centrifuged at 11,000 rpm for 12 min at 2-8°C. Tubes containing 500 µL of iso-

propyl alcohol were used to collect the supernatant of the different samples. Tubes were inverted 3 times and then incubated for 10 min at room temperature. To obtain RNA precipitate, samples were centrifuged at 11,000 rpm for 12 min at 2-8°C, and the supernatant was removed. Pellets were washed with 75% ethanol and centrifuged at 9,000 rpm for 5 min at 2-8°C. Then, the ethanol was removed, and the tubes were left at room temperature for 20 minutes to allow ethanol droplets to evaporate. The pellets were dissolved in 30 µL of RNase-free water and incubated for 30 min on ice. RNA purity and quantification were determined using Nanodrop (Thermo Fischer Scientific, Wilmington, DE, USA).

cDNA synthesis and RT-PCR: The cDNA strands were synthesized from mRNA using iScript advanced transcriptase from Bio-Rad. A combination of 4 µL of 5× iScript advanced reaction mix, 1 µL of reverse transcriptase, 5 µL of the sample (1.5 ug/reaction), and 10 µL of water were combined in a 0.2 mL tube in a total volume of 20 µL and vortexed for 30 sec. Reverse transcription was performed using the thermocycler program at 46°C for 20 min and 95°C for 1 min. For the RT-PCR amplification procedure, a mixture of 1 µL of the sample (200 ng cDNA/reaction), 10 µL of master mix, 1 µL of primer, and 8 µL of water was added to each well. The thermal cycling protocol included an initial holding step at 95°C for 2 min and denaturation at 95°C for 15 sec, followed by 40 cycles of 60°C for 30 sec (annealing/extension) and 60°C for 5 sec/step (melting curve) using the Bio-Rad CFX96 Real-Time System (Hercules, CA, USA). The individual primers used were specific to each gene of interest. The Unique Assay ID for the primers is described as follows: Nrf2 (qHsaCED0038543); KEAP1 (qHsaCID0017511); MUC1 (qHsaCED00198); JAK1 (qHsaCID000878); STAT3 (qHsaCID001091); NF-κB1 (qHsaCED00023); NF-κB2 (qHsaCED00198); CCL2 (qHsaCID0011608).

Capillary electrophoresis Wes analysis

For the determination of protein expression, treatments consisted of control (DMSO), IFN-γ (100 ng/mL), cardamonin (concentrations of 12.5 µM and 25 µM) + IFN-γ (100 ng/mL). The cells were treated with IFN-γ 1 h before adding cardamonin concentrations. At 24 hours of treatment, pellets were prepared, and a lysis buffer containing a protease inhibitor cocktail was added. Cells were sonicated with protease, centrifuged, and the supernatant was collected. Protein concentration was measured with the bicinchoninic acid (BCA) Protein Assay Kit (Item # 23225). Standards from 0 to 2000 µg/mL concentration, samples, and protein assay reagent were added to the 96-well plate. The Synergy H.T.X. Multi-Reader (BioTek, USA) was used to measure the concentration of proteins at 562 nm wavelength. Protein expression was determined using automated Wes™ ProteinSimple (San Jose, CA, USA). ProteinSimple provided reagents and plates, and the analysis was completed according to the protocol. The antibody and protein concentrations to be used were based on optimization experiments. Proteins were integrated with a master mix to obtain final concentrations of 0.25-1 mg/mL total protein, 1× sample buffer, 1× fluorescent molecular weight markers, and 40 mM dithiothreitol. For 5 min, samples were heated to 95°C. The blocking solution, samples, primary antibodies (dilution: 1:5 to 1:125), chemiluminescent substrate, horseradish peroxidase-conjugated secondary antibodies, and separation and stacking matrices were inserted into assigned wells into a microplate. The target protein was analyzed using a specific primary antibody, an HRP-conjugated secondary antibody, and a chemiluminescent substrate. The microplate was loaded and inserted into the instrument, and the fully automated electrophoresis and immunodetection were performed. The device camera captured Chemiluminescence, and the digital image was analyzed and quantified using the ProteinSimple Compass software (Wes-WS2709). Protein expression was normalized using GAPDH as the loading control, and the normalization was calculated using ProteinSimple Compass Software. The selected Cell Signaling antibody are described as follows: NRF2 (E3J1V) Rabbit mAb #33649; GAPDH (D16H11) XP® Rabbit mAb #5174.

ELISA

The effect of cardamonin on PD-L1 expression was investigated using a quantitative ELISA assay. The cells were treated with IFN-γ or TNF-α 1 h before adding cardamonin concentrations. Supernatants from control (DMSO), IFN-γ (100 ng/mL), TNF-α (50 ng/mL), and cardamonin + TNF-α (50 ng/mL) or IFN-γ (100 ng/

mL) treated cells were collected and centrifuged at 2,000×g for 10 minutes to remove debris. A volume of 100 µL of samples or standards was added to the wells and left for 2.5 h under gentle agitation. The plate was washed, 100 µL of antibody cocktail was added to the wells, and the plate was incubated for 1 h. After this, the plate was washed, 100 µL of streptavidin was added, and after 45 min of incubation, the substrate reagent was incubated for 30 min. After adding 50 µL of stock solution, the data was quantified by determining the optical density at 450 nm (Synergy HTX multi-Reader-BioTek, USA).

Data analysis

Statistical analysis was performed using GraphPad Prism (version 9.4.1) (San Diego, CA, USA). All data points were expressed as the mean ± SEM from 3 independent experiments, and the Statistical significance among the samples was calculated using a one-way ANOVA and Dunnett's multiple comparison tests (*P < 0.05, **P < 0.01, ***P < 0.001, and ****P < 0.0001, ns = P > 0.05). Gene expression analysis was performed with the CFX 3.1 Manager software (Bio-Rad, Hercules, CA), and the protein expression was analyzed with ProteinSimple Compass software - Wes-WS2709 (San Jose, CA 95134, USA). STRING (Search Tool for Retrieving Interacting Genes/proteins: https://string-db.org/ accessed on July 23, 2024) [37] database was utilized to display gene and protein interactions.

Results

Cardamonin cytotoxic effects

Cell viability was conducted using Alamar Blue® reagent at a 24-hour treatment period. TNBC cells were treated with cardamonin or co-treated with cardamonin and IFN-γ. A dose-response curve was observed as cardamonin concentrations increased (**Figure 1A** and **1B**). The cell viability of both cell lines showed no statistical difference after IFN-γ treatment compared to the control. In the MDA-231 cells, the co-treatment of cardamonin and IFN-γ did not cause any statistically significant changes in cell viability at cardamonin concentrations from 0.78 to 6.25 µM. However, as cardamonin concentration increased from 12.5 to 200 µM, a dose-response was observed (**Figure 1C**). In the MDA-468 cells, cardamonin concentrations of 0.78 and 1.56 µM did not cause any statistically significant effect; however, the concentrations from 3.12 to 200 µM induced a dose-response curve (**Figure 1D**). The IC50s calculated for both cell lines indicates that MDA-468 cells (38.1 ± 0.9 µM) are more sensitive to cardamonin effects compared to MDA-231 cells (57.4 ± 7.4 µM). Based on these results, we selected the concentrations of 12.5, 25.0, and 50.0 µM to be used in further experiments.

Cardamonin effects on cell morphology

A phase contrast microscope was used to analyze the effects of the different treatments on the cellular morphology of MDA-231 and MDA-468 cell lines at 24 h. Cells were photographed at 40× magnification. The treatments consisted of control (DMSO), IFN-γ (100 ng/mL), and concentrations of cardamonin ranging from 12.5-50 µM. In the MDA-231 cells, the control group was treated with DMSO (< 0.1%) and showed intact, long, and thin spindle-shaped cells (**Figure 2A**). The same treatment on the MDA-468 cells showed a mixture of rounded and long spindle-shaped cells (**Figure 2B**). The IFN-γ treatment did not cause any modification on the morphology of the cells in neither cell lines compared to the control, which was expected since the concentration used was not cytotoxic. In the MDA-231 cells, cardamonin induced noticeable morphological changes at the concentration of 50 µM, where cells shifted from a spindle to a small spherical shape. In the MDA-468 cells, the spindle-shaped cells disappeared after the treatment with 50 µM of cardamonin, and the cells displayed shrunken to smaller rounded cellular shapes (**Figure 2A** and **2B**).

Cardamonin effects on mRNA and protein expression of PD-L1

To investigate the effects of cardamonin on the mRNA expression of PD-L1, RT-PCR using PD-L1 individual primer was conducted. Data showed that MDA-231 cells exhibit a basal level of PD-L1 expression, which was not observed in the MDA-468 cells. In both MDA-231 and 468 cells, there was no increase in PD-L1 expression when cardamonin was tested in concentrations of 12.5, 25, and 50 µM, with levels of expression going lower than the control in the MDA-231 cells. The treatment with

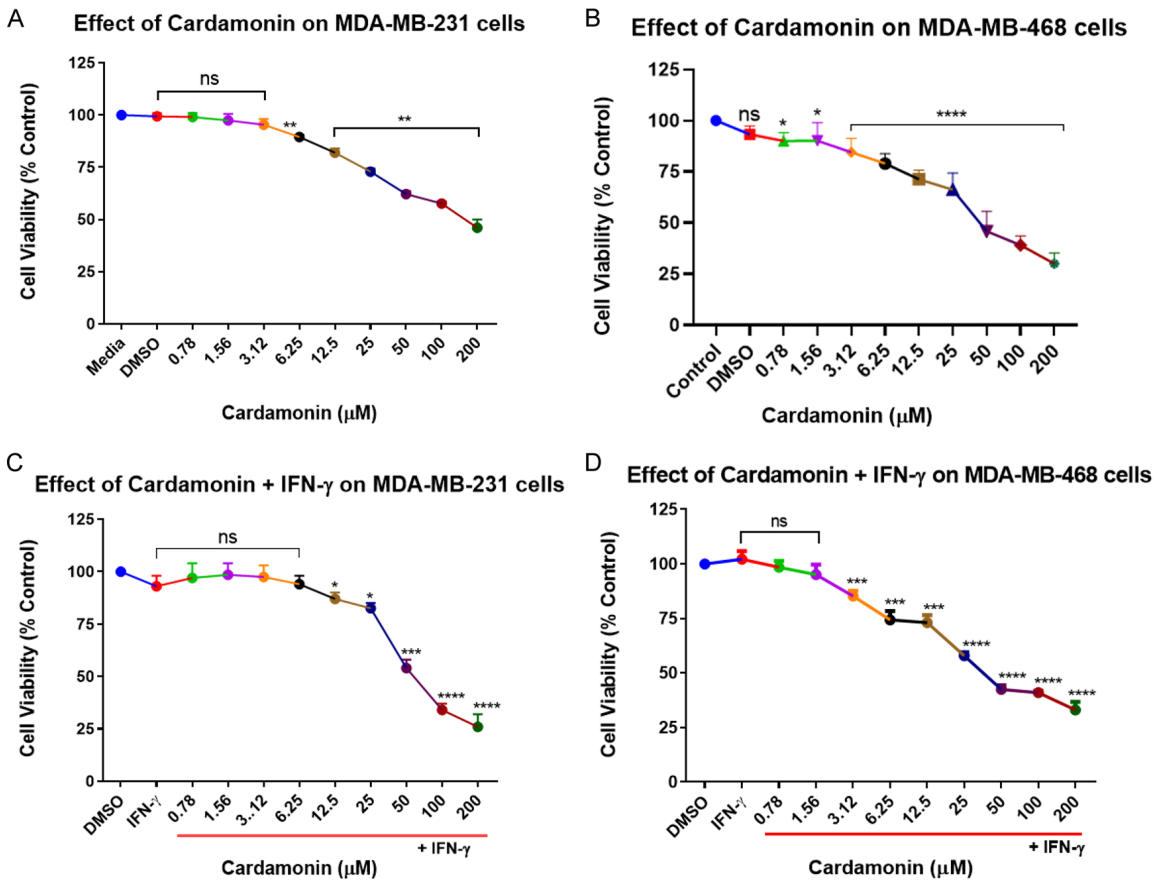

Figure 1. The effect of cardamonin on cell viability in MDA-231 (A and C) and MDA-468 (B and D) TNBC cells treated with cardamonin only or co-treated with cardamonin and IFN-γ (100 ng/mL). The concentration range of cardamonin varied from 0.78-200 μM, and the control cells were treated with DMSO (< 0.1%). Each experiment was performed 3 times with n = 5 at 5% CO_2 and 37 °C. The cytotoxic effect was measured over a 24-h period. The data are presented as the mean ± SEM. Statistical significance between control vs. treatments was evaluated by a one-way ANOVA, followed by Dunnett's multiple comparison tests. *P < 0.05, **P < 0.01, ***P < 0.001, ****P < 0.0001, ns = P > 0.05.

IFN-γ caused an increase in PD-L1 expression by 4-fold in the MDA-231 and by 20-fold in the MDA-468 cells at 24 h, compared to the control. When cells were co-treated with cardamonin and IFN-γ, there was a concentration-dependent decrease in the expression of PD-L1 (**Figure 3A** and **3B**). In MDA-231 cells, there was a 74% inhibition on the mRNA expression of PD-L1, and in MDA-468 cells, a decrease of 84%, showing a higher inhibition of PD-L1 in the MDA-468 cells. To confirm the results at the protein level, ELISA kits specific for PD-L1 were used to investigate the effect of cardamonin on the expression of PD-L1. The results showed a high protein expression of PD-L1 after IFN-γ treatment and a decrease in PD-L1 expression with the co-treatment, confirming the data on the transcription level. In MDA-231 cells, at the highest concentration of cardamonin (50 μM), the protein expression of PD-L1 was inhibited by 59%, and in MDA-468 cells, the inhibition of PD-L1 protein expression reached 100% (**Figure 3C** and **3D**).

Cardamonin effects on Nrf2 and Keap1 mRNA expression

In this study, Nrf2 and Keap1 mRNA expressions were investigated in both cell lines using RT-PCR with individual primers. The data showed that cardamonin increased Nrf2 expression in the MDA-231 cells but not in the MDA-468 cells compared to the control. The IFN-γ treatment did not cause any increase in the mRNA expression of Nrf2 in either one of the cell lines at 24 h, compared to the control. However, when cardamonin was co-treated with IFN-γ, there was a significant increase in

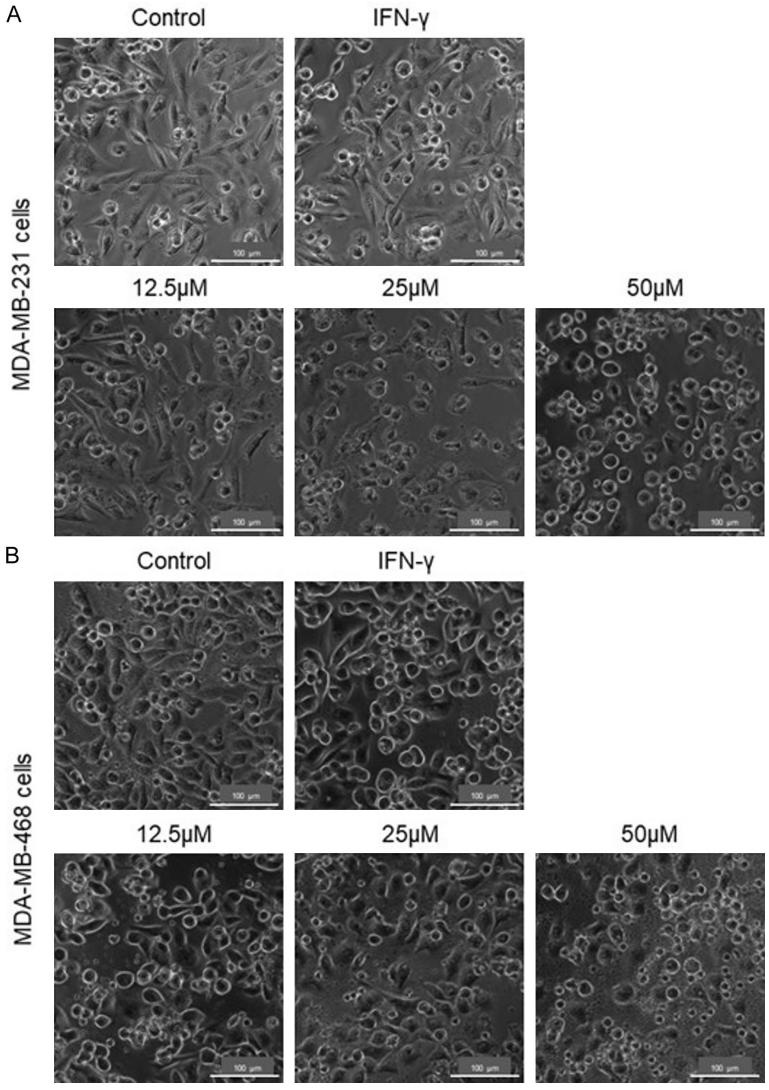

Figure 2. Morphological changes induced by cardamonin on MDA-231 (A) and MDA-468 (B) TNBC cells. Morphological changes induced by cardamonin (12.5-50 μM) in MDA-231 and MDA-468 cells were photographed at 24 h. Cells were visualized using phase contrast and photographed at 40× magnification. Images were captured using the Olympus Cell Sens Standard Cytation5 cell Imaging reader (BioTek Instruments, Inc., Winooski, VT, USA).

the Nrf2 expression at the concentration of 25.0 μM in the MDA-231 and concentrations of 25 and 50.0 μM in the MDA-468 cells (**Figure 4A** and **4B**). When analyzing the effect of cardamonin in Keap1 expression, the results showed an increase in the MDA-231 cells at the concentration of 25 μM and in the MDA-468 at the concentration of 12.5 and 25 μM. The co-treatment with IFN-γ showed no significant increase in the mRNA expression of Keap1 in the MDA-231 cells, but there was a 1.7-fold increase in the MDA-468 cells. The co-treatment with cardamonin and IFN-γ revealed that one concentration of cardamonin (12.5 μM) induced the expression of Keap1 in MDA-231. Still, in the MDA-468 cells, 12.5 and 25 μM concentrations showed a statistically significant effect compared to the control (**Figure 4C** and **4D**).

Cardamonin effects on Nrf2 protein expression

To investigate the effect of cardamonin on Nrf2 protein expression, capillary electrophoresis, Wes analysis was performed with a specific antibody against total Nrf2 protein. The data demonstrated that the activation with IFN-γ did not cause any significant change in the protein expression of Nrf2 in either cell line compared to the control. However, at 25 μM, cardamonin significantly increased the Nrf2 protein expression in both cell lines in the presence of IFN-γ at a 24-h treatment period. These data confirm the results obtained at the transcription level, showing an increase in Nrf2 expression in both MDA-231 and MDA-468 TNBC cells at the concentration of 25 μM (**Figure 5A-D**).

Cardamonin effects on the mRNA expression of PD-L1 inducers

To investigate a possible mechanism for the inhibitory effects of cardamonin on the expression of PD-L1, RT-PCR assays were conducted with specific primers for MUC1, JAK1, and STAT3, which are genes that modulate PD-L1 activation. The results showed that the cardamonin effect modulated the expression of these genes differently. The IFN-γ treatment induced the expression of all the genes except for JAK1 on the MDA-468 cells (**Figure 6D**), which had no statistically significant increase in the expression levels compared to the control. In the MDA-231 cells, the co-treatment of IFN-γ

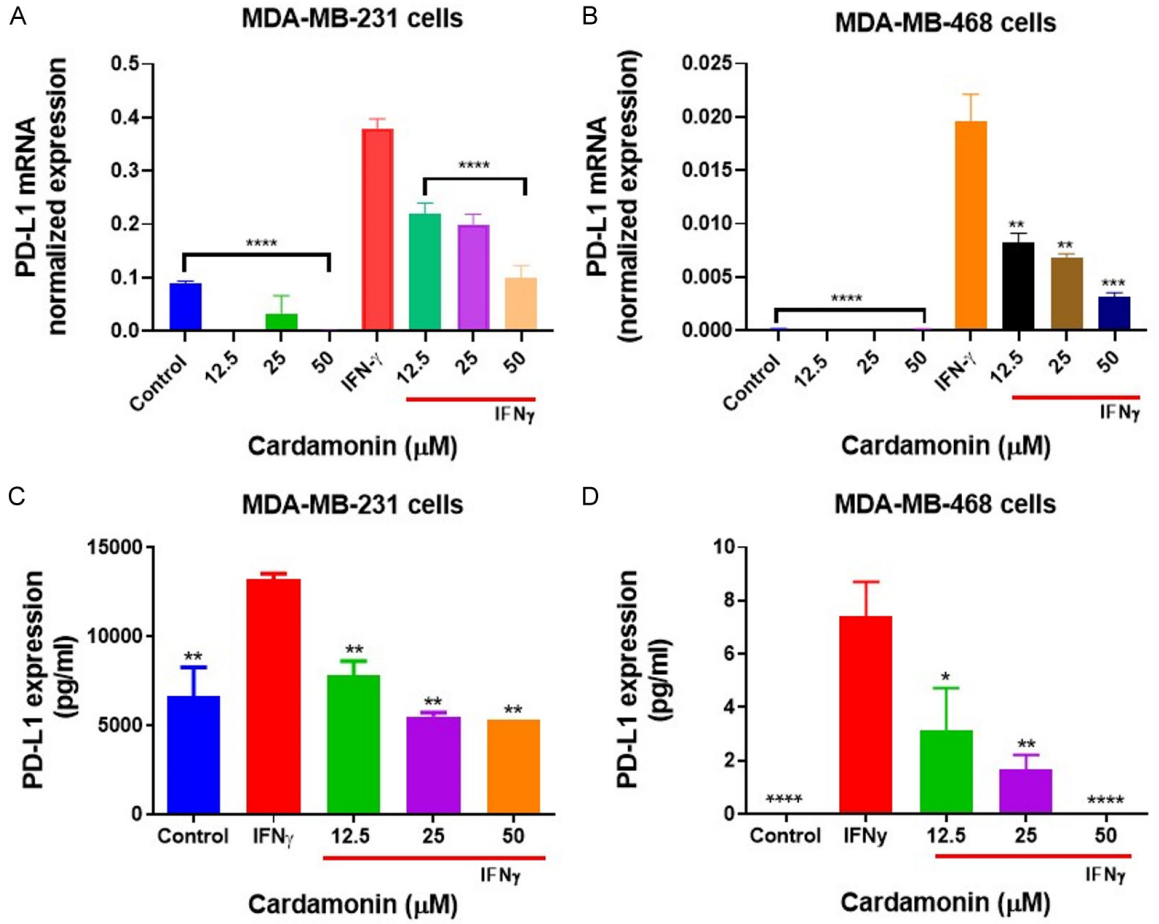

Figure 3. The effect of cardamonin on normalized mRNA (A and B) and protein expression of PD-L1 (C and D) in MDA-231 (A and C) and MDA-468 (B and D) TNBC cells. Concentrations of cardamonin tested were in the range of 12.5-50 μM with or without IFN-γ (100 ng/mL), and control cells were treated with DMSO (< 0.1%). Each experiment was performed 3 times with n = 5 at 5% CO_2 and 37°C. The data are presented as the mean ± SEM. Statistical significance between IFN-γ vs. treatments was evaluated by a one-way ANOVA, followed by Dunnett's multiple comparison tests. *P < 0.05, **P < 0.01, ***P < 0.001, ****P < 0.0001, ns = P > 0.05.

and cardamonin promoted a statistically significant decrease in the mRNA expression of MUC1, JAK1, and STAT3 expression, compared to IFN-γ treatment alone (**Figure 6A**, **6C**, **6E**). In the MDA-468 cells, the co-treatment caused a reduction in the mRNA expression of MUC1 and STAT3. However, there was an increase in the expression of JAK1 compared to IFN-γ treatment alone (**Figure 6B**, **6D**, **6F**).

Furthermore, the inhibitory effect of cardamonin on genes that activate the NF-κB signaling was also investigated using RT-PCR assay with specific primers. Treatment with cardamonin modulated the expression of NF-κB1 (p50) and NF-κB2 (p52) in MDA-231 and MDA-468 cells. The data showed that IFN-γ treatment induced the expression of NF-κB1 but not NF-κB2 in both cell lines (**Figure 6G-J**). After cardamonin treatment, the MDA-231 cells showed a reduced expression of NF-κB1 in concentrations from 12 to 50 μM and in the MDA-468 cells, concentrations from 12.5 to 50 μM of cardamonin caused an inhibition of 50% in the expression of NF-κB1, compared to IFN-γ treatment (**Figure 6G** and **6I**). Even though IFN-γ treatment did not cause any statistically significant increase in NF-κB2 expression, cardamonin (50 μM) reduced levels of NF-κB2 to lower than the basal levels observed in the control of the MDA-231 cells, while having no significant effect on the MDA-468 cells (**Figure 6H** and **6J**).

Cardamonin effect on the mRNA and protein expression of CCL2

The effect of cardamonin on the gene and protein expression of CCL2 was investigated using

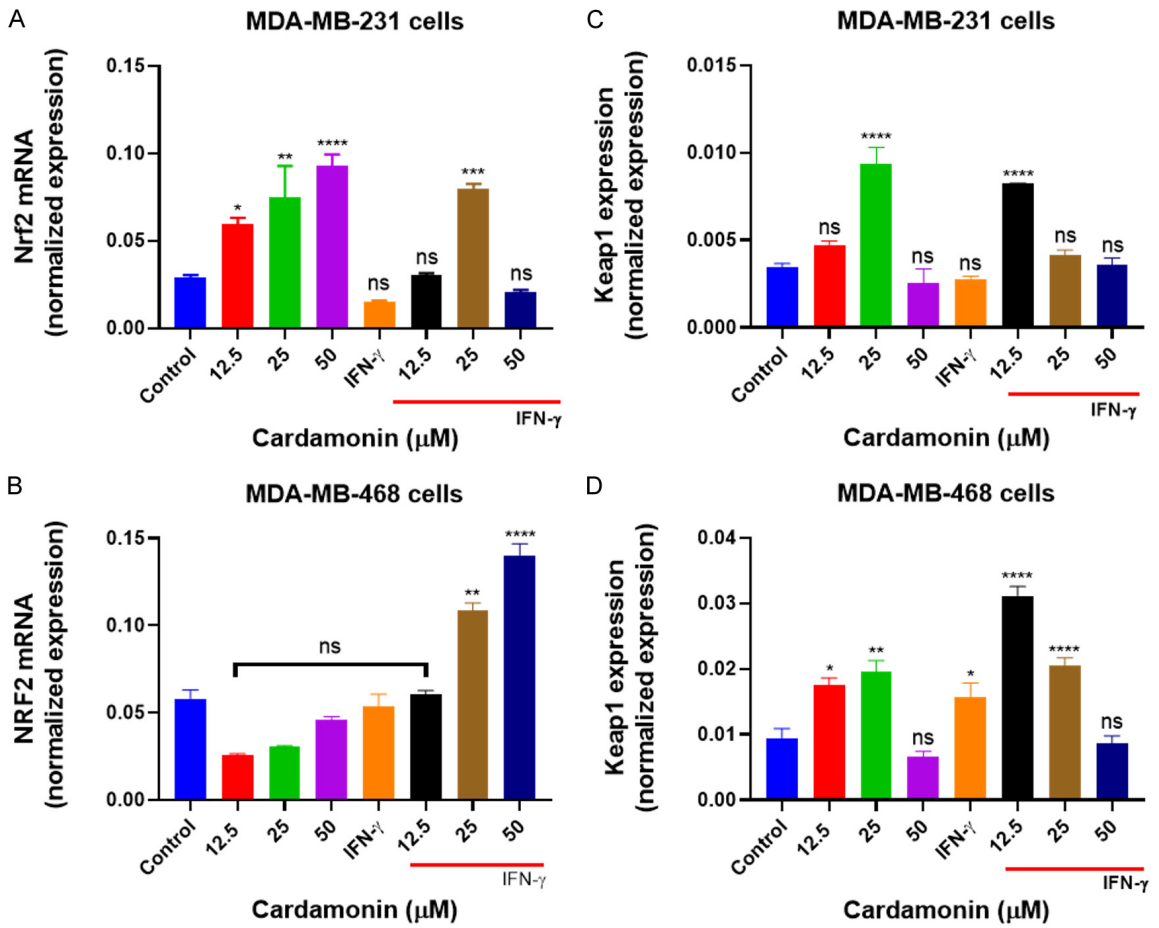

Figure 4. The effect of cardamonin on Nrf2 (A and B) and Keap1 (C and D) normalized mRNA expression in MDA-231 (A and C) and MDA-468 (B and D) TNBC cells. Concentrations of cardamonin tested were in ranges from 12.5-50 μM with or without IFN-γ (100 ng/mL), and the control cells were treated with DMSO (< 0.1%). Each experiment was performed 3 times with n = 5 at 5% CO_2 and 37 °C. The data are presented as the mean ± SEM. Statistical significance between control vs. treatments was evaluated by a one-way ANOVA, followed by Dunnett's multiple comparison tests. *P < 0.05, **P < 0.01, ***P < 0.001, ****P < 0.0001, ns = P > 0.05.

TNF-α to stimulate the cells. The data show that TNF-α in the concentration of 50 ng/mL induce the expression of CCL2 and does not present cytotoxicity [38, 39]. The RT-PCR assay data showed that TNF-α induced the expression of CCL2, showing a 5-fold increase in the MDA-231 cells and a 150-fold increase in the MDA-468 cells. With the combination of TNF-α and cardamonin, there was a decrease of 21-fold in the mRNA expression of CCL2 in the MDA-231 and a 159-fold decrease in the MDA-468 cells (**Figure 7A** and **7B**). At the protein level, TNF-α induced a 5-fold increase in the expression of CCL2 in the MDA-231 cells and a 43-fold increase in the MDA-468 cells compared to the control. When cardamonin and TNF-α were combined, there was a 3 and 5-fold decrease in CCL2 protein expression in the MDA-231 and MDA-468 cells, respectively, compared to TNF-α alone (**Figure 7C** and **7D**). These results show that CCL2 mRNA expression was inhibited by more than 90%, returning to control levels or less, and CCL2 protein expression was reduced by more than 60% after cardamonin treatment in both cell lines.

Functional enrichment analysis of proteins (STRING)

The bioinformatics tool STRING integrated all predicted associations between genes and proteins investigated in the present study, including functional associations and physical interactions. STRING is a proteomic database that uses computational prediction, experimental data, and scientific literature. This database

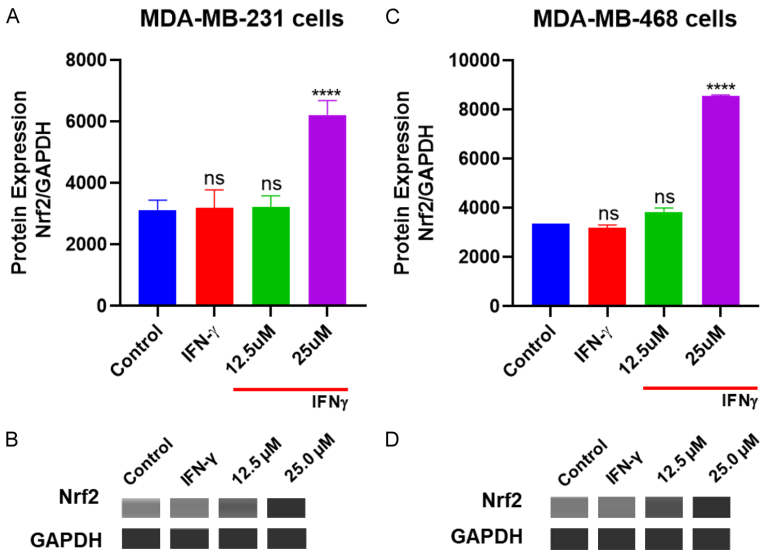

Figure 5. The effect of cardamonin on Nrf2 protein expression (A and C) in MDA-231 and MDA-468 TNBC cells. Bands (B and D) represent the protein expression of four treatments at 24 h. A one-way ANOVA evaluated the statistical significance between control vs. all treatments and control vs. treatments, followed by Dunnett's multiple comparison test. ns = non-significant, ***P < 0.001.

was used to perform the functional enrichment and association analysis of PD-L1, Nrf2, CCL2, MUC1, JAK1, and STAT3. The network displayed the direct interaction between genes and proteins with predicted functional partners (**Figure 8**). Each interaction scored from zero to one. According to the available evidence, the numbers showed the probability of interaction if it exists. The thickness of the edges showed protein-protein association confidence levels from lowest to highest (0.150-0.900). The figure does not show the finest line representing low interaction since all the interactions surpassed the lowest confidence index. There was a medium level of association between CCL2 and MUC1 (0.414), and the highest interaction occurred between JAK1 and STAT3 (0.999), confirming strong interaction between the genes and proteins selected in this study (**Table 1**).

Discussion

Recent studies have highlighted the critical role of the TIME in BC development, progression, and response to immunotherapy. TIME comprises a complex network of immune cells, signaling molecules, and stromal components that can either induce or reduce tumor growth [5, 40], and other non-malignant cells surrounding the tumor, plus a complex signaling molecule network that endures the internal connections of the microenvironment, including growth factors, cytokines, chemokines, and exosomes [41, 42]. This association between tumor cells and their immune microenvironment is crucial in cancer proliferation, propagation, and therapy response [43]. One essential means of survival is tumor immune escape, when cells avoid recognition and attack by the immune system, allowing them to grow and metastasize [44]. Also, tumor cells exploit immune checkpoints, such as PD-1/PD-L1, to suppress T cell activity and evade immune surveillance [45].

PD-L1 binding to the receptor inhibits T-cell activation and is considered a key contribution to immune resistance in the TIME [46]. PD-1 and tumor-infiltrating lymphocytes (TILs) relate to worse overall survival in patients with BC [47, 48]. At the same time, high levels of PD-L1 were reported with increased levels of TILs and high-grade hormone receptor-negative, HER2 overexpressed tumors and TNBCs [49]. Compared to other subtypes, TNBC has a higher rate of PD-L1 expression, providing a potential therapeutic target with antibody inhibitors of PD-1 or PD-L1 [50, 51]. Therefore, blocking the PD-1/PD-L1 axis has become a promising direction to halt immune suppression and reinstate the function of the immune system [13, 16]. However, it was demonstrated that even by blocking the binding of PD-L1 with PD-1 completely with PD-L1/PD-1 inhibitors, the overexpression of CCL2 by PI3K/AKT and NF-κB activation still may induce PD-L1/PD-1 inhibitors resistance by preventing cytotoxic T cell tracking towards to tumor [12]. The expression of these immune checkpoint molecules is often upregulated in response to inflammatory signals within the TIME, further inhibiting T-cell activation and function. Meanwhile, tumors can also induce immunosuppression through the regulatory T cells (Tregs), myeloid-derived suppressor cells (MDSCs), and cytokines (e.g., TGF-

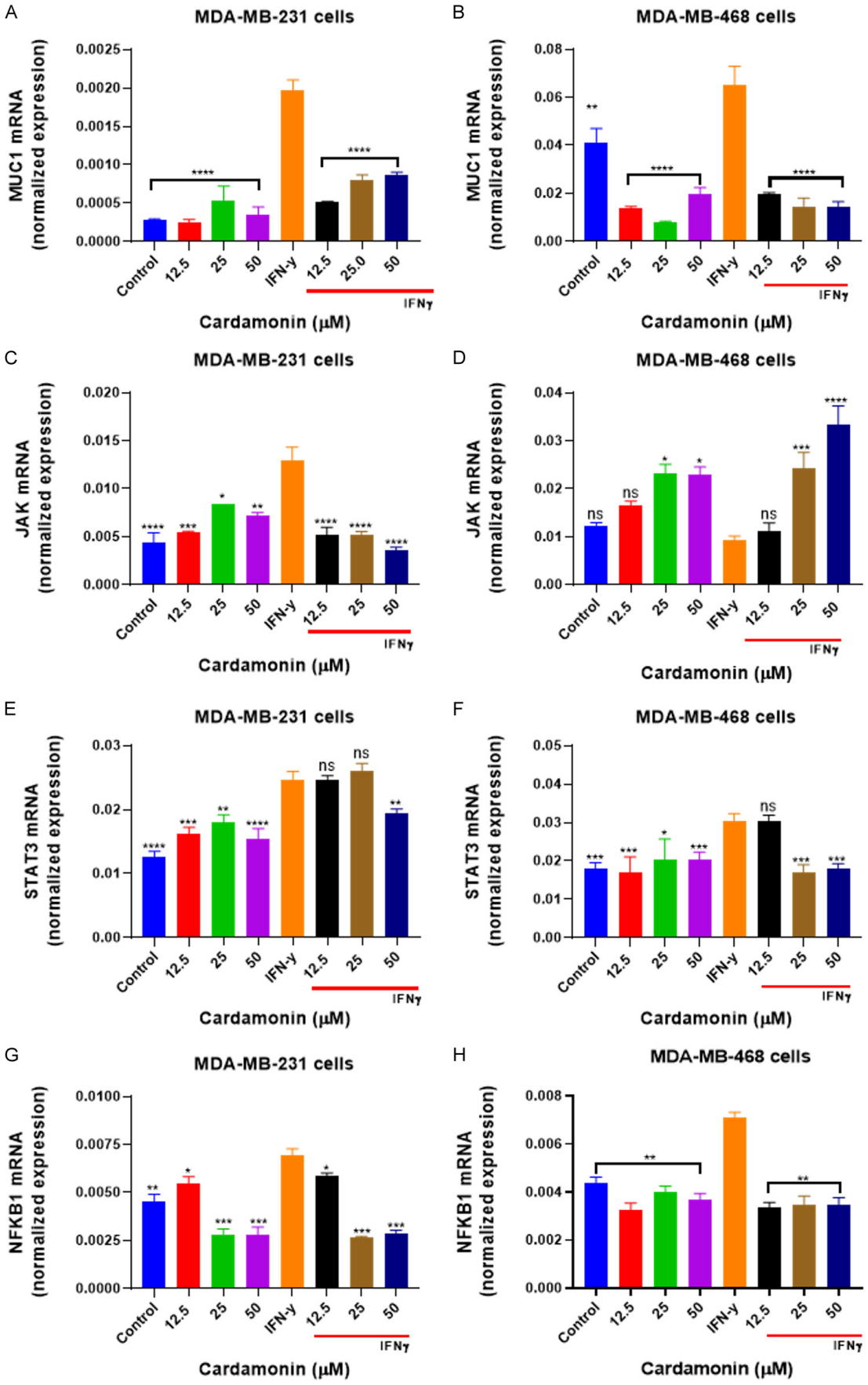
A
MDA-MB-231 cells
MUC1 mRNA (normalized expression)
Control
12.5
25
50
IFN-γ
12.5
25.0
50
IFNγ
Cardamonin (μM)
B
MDA-MB-468 cells
MUC1 mRNA (normalized expression)
Control
12.5
25
50
IFN-γ
12.5
25
50
IFNγ
Cardamonin (μM)
C
MDA-MB-231 cells
JAK mRNA (normalized expression)
Control
12.5
25
50
IFN-γ
12.5
25
50
IFNγ
Cardamonin (μM)
D
MDA-MB-468 cells
JAK mRNA (normalized expression)
Control
12.5
25
50
IFN-γ
12.5
25
50
IFNγ
Cardamonin (μM)
E
MDA-MB-231 cells
STAT3 mRNA (normalized expression)
Control
12.5
25
50
IFN-γ
12.5
25
50
IFNγ
Cardamonin (μM)
F
MDA-MB-468 cells
STAT3 mRNA (normalized expression)
Control
12.5
25
50
IFN-γ
12.5
25
50
IFNγ
Cardamonin (μM)
G
MDA-MB-231 cells
NFKB1 mRNA (normalized expression)
Control
12.5
25
50
IFN-γ
12.5
25
50
IFNγ
Cardamonin (μM)
H
MDA-MB-468 cells
NFKB1 mRNA (normalized expression)
Control
12.5
25
50
IFN-γ
12.5
25
50
IFNγ
Cardamonin (μM)

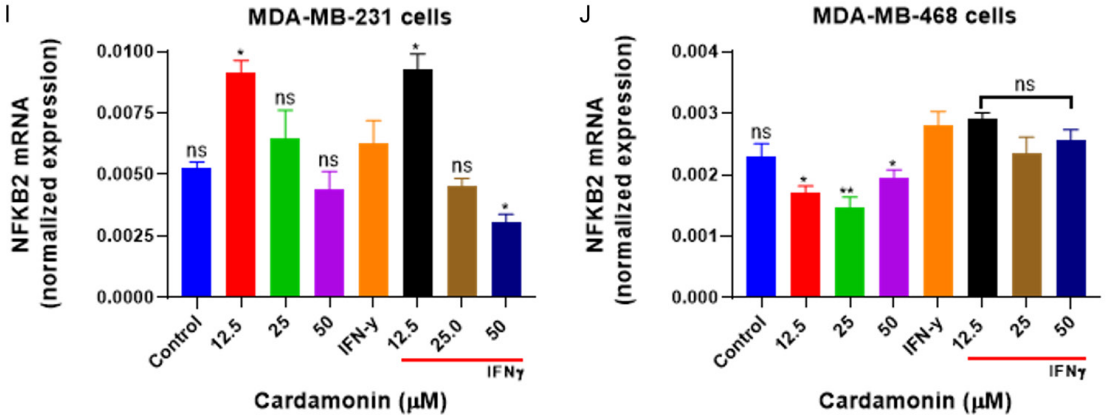

Figure 6. The effect of cardamonin on normalized mRNA expression of MUC1 (A and B), JAK1 (C and D), STAT3 (E and F), NF-κB1 (G and H), and NF-κB2 (I and J) in MDA-231 and MDA-468 TNBC cells. Concentrations of cardamonin tested were in the range of 12.5-50 μM with or without IFN-γ (100 ng/mL), and the control cells were treated with DMSO (< 0.1%). Each experiment was performed 3 times with n = 5 at 5% CO_2 and 37 °C. The data are presented as the mean ± SEM. Statistical significance between IFN-γ vs. treatments was evaluated by a one-way ANOVA, followed by Dunnett's multiple comparison tests. *P < 0.05, **P < 0.01, ***P < 0.001, ****P < 0.0001, ns = P > 0.05.

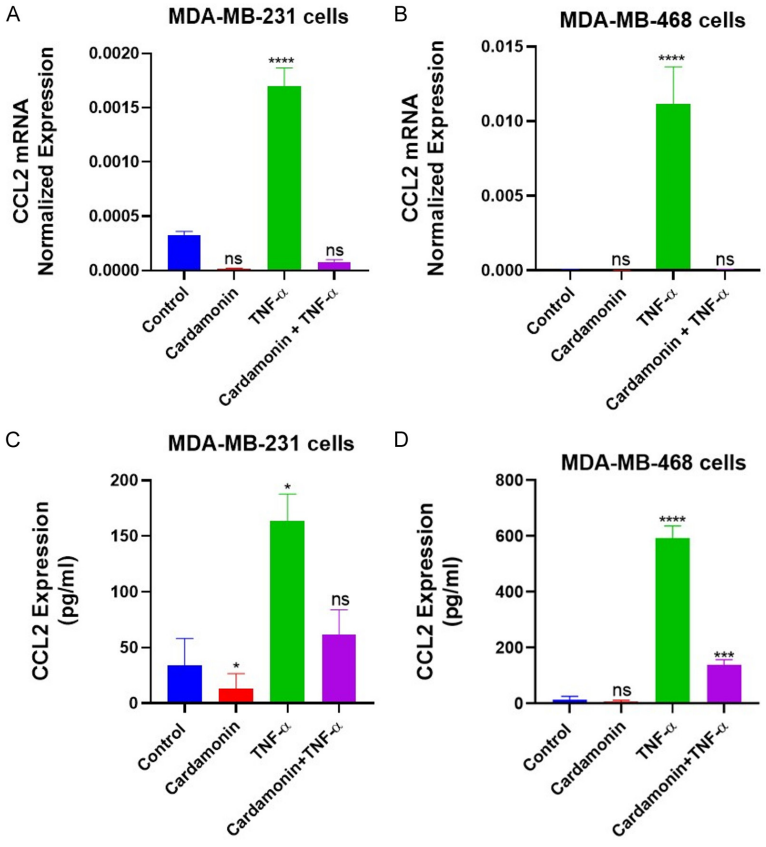

Figure 7. The effect of cardamonin on normalized mRNA (A and B) and protein expression of CCL2 (C and D) in MDA-231 and MDA-468 TNBC cells. The concentration of cardamonin used was 12.5 μM with or without TNF-α (50 ng/mL), and the control cells were treated with DMSO (< 0.1%). Each experiment was performed 3 times with n = 5 at 5% CO_2 and 37 °C. The data are presented as the mean ± SEM. Statistical significance between control vs. treatments was evaluated by a one-way ANOVA, followed by Dunnett's multiple comparison tests. *P < 0.05, **P < 0.01, ***P < 0.001, ****P < 0.0001, ns = P > 0.05.

β) to create an immunosuppressive microenvironment [45]. Moreover, tumors can secrete immunosuppressive factors (e.g., IL-10, VEGF) that inhibit immune responses [45].

Currently, the FDA-approved immune checkpoint inhibitors (atezolizumab, avelumab, and durvalumab) targeting the PD-1/PD-L1 pathway require the measurement of PD-L1 [52]. Since 2019, atezolizumab has been used in combination with protein-bound paclitaxel in patients whose tumors express PD-L1 for metastatic TNBC [53]. However, because of the low efficacy and numerous undesirable side effects along with the treatment [52], there is a need to find combinatory therapies that could be more efficient and with fewer toxic effects. For this reason, this study investigated the effect of the flavonoid cardamonin on the expression of PD-L1 in the stimulated TNBC cells and found that PD-L1 levels differ between the MDA-231 and MDA-468 cells after

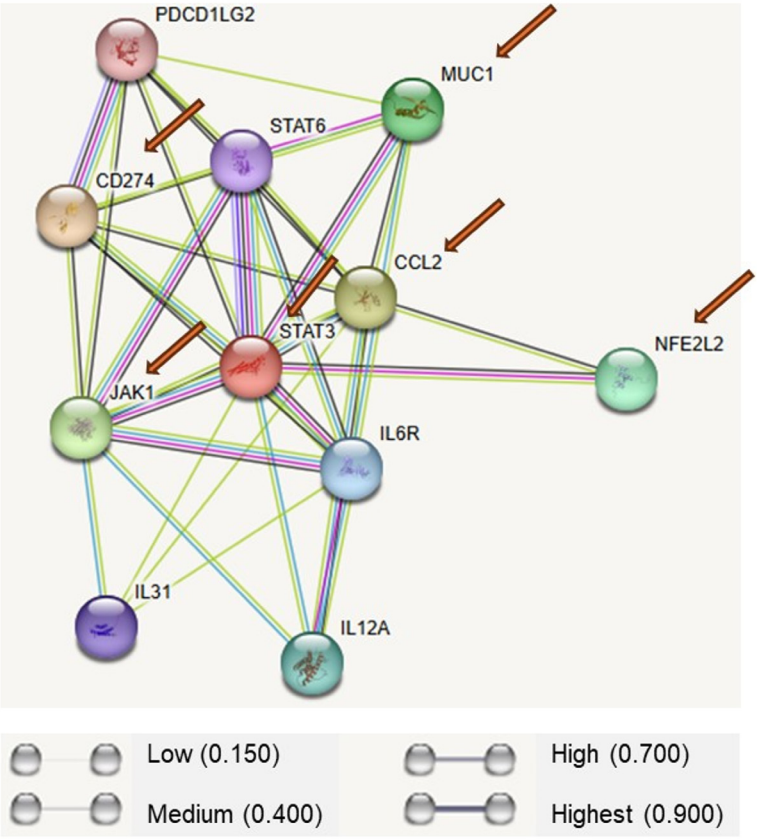

Figure 8. Functional Enrichment Analysis (STRING) of PD-L1 (CD274), Nrf2 (NFE2L2), CCL2, MUC1, JAK1, and STAT3 with predicted functional interaction. The legend displays edges representing protein-protein associations and the confidence index representing the probability of interactions.

stimulation. However, these levels were reduced with cardamonin treatment.

The IFN-γ/JAK/STAT signaling pathway was also investigated since this pathway has been reported to induce PD-L1 expression in several cancers [54-56]. The data showed that cardamonin treatment decreased the mRNA expression of JAK1 and STAT3 in the stimulated MDA-231 cells, differing from the MDA-468 cells, where just STAT3 levels were decreased. Studies show that in the TIME, infiltrated T lymphocytes can activate the JAK/STAT signaling pathway after IFN-γ stimulation [57], which may induce the expression of PD-L1. Literature has also implied that dysregulated JAK/STAT signaling represents a promising therapeutic target for the modulation of immune responses [58]. Likewise, JAK1/JAK2 mutations blocked PD-L1 induction, protecting cancer cells from the immune system attack [59]. In concordance with the present study's findings, these results suggest that inhibiting the JAK/STAT signaling pathway may improve the efficacy of PD-L1 inhibitors in immunotherapy. However, additional research is needed to confirm this hypothesis.

To further investigate the cardamonin molecular mechanism in inhibiting PD-L1 expression, the present study also evaluated its effect on Mucin1 (MUC1) expression, which is overexpressed in about 90% of TNBCs [60]. The results showed that cardamonin treatment significantly decreased MUC1 levels in both stimulated TNBC cell lines. MUC1 works as an oncoprotein that interacts with many effectors associated with the hallmarks of cancer cells [60]. The MUC1-C subunit integrates multiple signaling pathways at the membrane and nucleus of the cells [60, 61]. Therefore, MUC1-C activates PI3K/AKT and MEK/ERK signaling in TNBC and other BC cells [62, 63]. It also directly activates the β-catenin→TCF4→MYC and NF-κB p65 pathways, thereby inducing the transcription of target genes [62, 64]. Studies showed that MUC1 overexpression, and particularly the oncogenic MUC1-C subunit, by cancer cells is related to protection from killing by TRAIL, Fas ligand, and T-cell perforin/granzyme B-mediated lysis [65, 66], supporting the concept that MUC1-C contributes to immune evasion. The oncogenic MUC1-C targeting was sufficient to suppress PD-L1 expression in TNBC cells, showing that MUC1-C increased PD-L1 transcription by recruiting MYC and NF-κB p65 to the PD-L1 promoter [67]. Therefore, the literature agrees with the results of this study, showing that MUC1 would also be a valuable target to decrease the levels of PD-L1 and to reduce activation of NF-κB signaling.

NF-κB is a proinflammatory transcription factor normally overactivated in BC. It enables the growth of a hormone-independent, invasive,

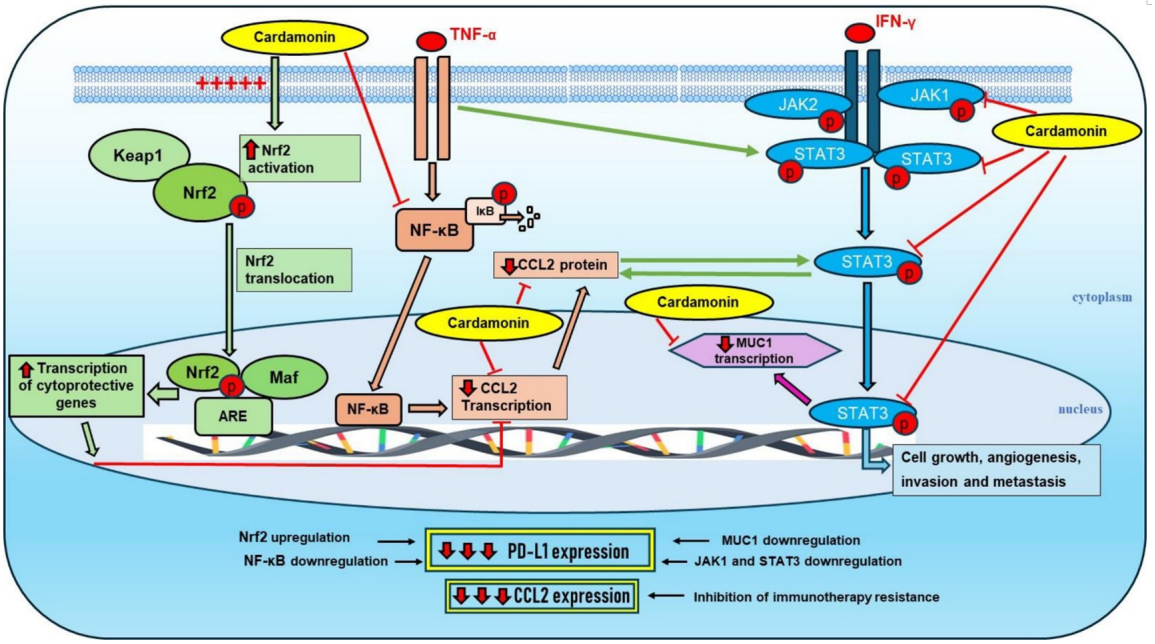

Figure 9. Summary of the anticancer molecular mechanisms of cardamonin. The figure describes the cardamonin effect on the upregulation of Nrf2 expression and downregulation of NF-κB, MUC1, JAK1, STAT3, and CCL2 expression.

Table 1. The table displays the interaction scores

Node1	Node2	Node1 Accession	Node 2 Accession	Score
CCL2	PD-L1 (CD274)	ENSP00000225831	ENSP00000370989	0.690
CCL2	JAK1	ENSP00000225831	ENSP00000499900	0.781
CCL2	MUC1	ENSP00000225831	ENSP00000484824	0.414
CCL2	Nrf2 (NFE2L2)	ENSP00000225831	ENSP00000380252	0.581
CCL2	STAT3	ENSP00000225831	ENSP00000264657	0.867
CD274	CCL2	ENSP00000370989	ENSP00000225831	0.690
CD274	JAK1	ENSP00000370989	ENSP00000499900	0.603
CD274	MUC1	ENSP00000370989	ENSP00000484824	0.597
CD274	STAT3	ENSP00000370989	ENSP00000264657	0.992
JAK1	CCL2	ENSP00000499900	ENSP00000225831	0.781
JAK1	PD-L1 (CD274)	ENSP00000499900	ENSP00000370989	0.603
JAK1	STAT3	ENSP00000499900	ENSP00000264657	0.999
MUC1	CCL2	ENSP00000484824	ENSP00000225831	0.414
MUC1	PD-L1 (CD274)	ENSP00000484824	ENSP00000370989	0.597
MUC1	STAT3	ENSP00000484824	ENSP00000264657	0.752
NFE2L2	CCL2	ENSP00000380252	ENSP00000225831	0.581
NFE2L2	STAT3	ENSP00000380252	ENSP00000264657	0.742
STAT3	CCL2	ENSP00000264657	ENSP00000225831	0.867
STAT3	PD-L1 (CD274)	ENSP00000264657	ENSP00000370989	0.992
STAT3	JAK1	ENSP00000264657	ENSP00000499900	0.999
STAT3	MUC1	ENSP00000264657	ENSP00000484824	0.752
STAT3	Nrf2 (NFE2L2)	ENSP00000264657	ENSP00000380252	0.742

The numbers in red color represent the highest probabilities of interaction.

high-grade, and late-stage tumor phenotype [68] through abnormal constitutive expression of NF-κB subunits (such as c-Rel, p65, and p50), which have been extensively reported in BCs [69]. The current investigation showed that cardamonin decreased the levels of NF-κB1 and NF-κB2 in the stimulated MDA-231 cells, but in the MDA-468, just the expression of NF-κB1 was reduced, indicating that the molecular mechanism of cardamonin may differ depending on the cell genetics and its origin. The results suggest that cardamonin may decrease PD-L1 levels through inhibition of MUC1 and subsequent reduction in the expression of NF-κB1 (p50) and NF-κB2 (p52), which modulate the activation of the NF-κB signaling and further transcription of inflammatory cytokines.

These inflammatory cytokines function as TIME regulators, representing the main communication bridge between cancer cells, the tumor stroma, and the immune system. Chemokines and chemokine receptors were strongly correlated with cancer-associated chronic inflammation and were considered responsible for the recruitment of immune cells. More recent studies indicate elevated levels of CCL2 in tumor tissue, providing further evidence that CCL2 may lead to tumor spreading and the development of a pre-metastatic niche [7]. Moreover, CCL2 is the cytokine investigated in human BC tissues, cell lines, and animal BC models, and the results show the crucial involvement of CCL2 in the metastasis of BC [70]. Meanwhile, cytokines play a significant role in the expression of PD-L1 and the activation of immune cells [71].

Furthermore, cancer cells dynamically secrete CCL2 due to genetic mutations and metabolic dysfunction. Likewise, cancer chemotherapy and radiotherapy also stimulate CCL2-dependent chronic inflammation and tumor survival [7]. In the present study, cardamonin treatment reduced the CCL2 mRNA expression 21-fold in the stimulated MDA-231 cells and caused a remarkable downregulation of 159-fold in the MDA-468 cells. Cardamonin reduced CCL2 expression by more than 60% at the protein level. CCL2 is an inflammatory cytokine that induces the enrollment of macrophages in the TIME [72], which may diminish the effect of the PD-1/PD-L1 inhibitor by postponing infiltration of T cells, such as CD8+ cytotoxic T cells [73]. The increase in CCL2-macrophage recruitment can induce resistance to immunotherapy by reducing the infiltration of cytotoxic T cells into the tumor. Therefore, CCL2 is considered a crucial target in cancer immune treatment because it induces cancer growth through angiogenesis in the TIME and reduces infiltration of cytotoxic T cells, reducing immunotherapy treatment efficiency [88]. Cytokines such as CCL2 help suppress antitumor immunity and can prevent the cytotoxic effects of CD8+ T cells [74]. Therefore, targeting cytokines, such as CCL2, in combination with PD-1/PD-L1 inhibition may lead to an increase in T-cell infiltration, antitumor immunity, and a reduction in tumor resistance to immunotherapy [75], improving the efficacy and decreasing the resistance against immunotherapies [76]. Therefore, the results of this investigation corroborate with the literature, suggesting that cardamonin may help enhance the efficacy of TNBC treatments and reduce immunotherapy resistance by lowering the levels of CCL2.

Moreover, our study investigated the effect of cardamonin on the activation of Nrf2, which induces the transcription of antioxidant genes that were reported to block the expression of CCL2 and other inflammatory mediators [77]. The findings showed that cardamonin significantly increased Nrf2 expression in both stimulated TNBC cell lines. Literature reported that peritoneal neutrophils from Nrf2-knockout mice treated with LPS presented increased levels of cytokines (TNF-α and IL-6) and chemokines (CCL2 and MIP2) compared to wild-type cells [77]. The transferring of the Nrf2 gene to human and rabbit aortic smooth muscle cells in vitro suppressed CCL2 secretion [78, 79], and the expression of Nrf2-dependent HO-1 suppressed TNF-α-stimulated NF-κB and CCL2 secretion in human umbilical vein endothelial cells [80]. This data indicates that, in response to inflammatory stimuli, upregulation of Nrf2 signaling helps to inhibit the overproduction of proinflammatory cytokines and chemokines and limits NF-κB activation [80]. However, continued activation of Nrf2 has been reported as a driver of the malignant progression of many types of cancers, and its function in BC is still controversial due to conflicting data.

In the last decade, numerous studies have reported that activation of Nrf2 in cancer cells induces cancer progression [81-83] and metas-

tasis [84], conferring resistance to chemo- and radiotherapy [85, 86]. However, with the support of updated technologies and the discovery of new Nrf2 functions, understanding its roles in the diverse stages of cancer development has advanced significantly. Nrf2 directly upregulates its target genes or indirectly functions as a redox modulator in each cancer hallmark [87, 88]. Nrf2 was also described as a cytoprotective transcription factor with positive and negative effects on cancer [89, 90], protecting both normal and cancerous cells from oxidative damage, which means that it inhibits malignant transformation; however, once cancer is developed, it resists therapy [91]. This dual role in cancer is also observed with the NF-κB signaling pathway, where DNA damage occurs, causing cell death. Still, as cancer progresses, it sets numerous cancer hallmarks, including resistance to chemotherapy through cytokine overexpression, as observed with CCL2 [92]. Nrf2 counteracts the NF-κB action using various mechanisms, such as stimulation of antioxidant genes, impairment of the NF-κB signaling pathway, and decreased proinflammatory cytokine production [93]. These studies indicate that the increased expression of Nrf2 by cardamonin may be beneficial not only due to a direct effect on the activation of Nrf2 signaling, which is still controversial, but also because of indirect effects on NF-κB signaling and CCL2 release, which are connected to increased expression of PD-L1 and resistance to therapy.

The data presented in this study indicates that flavonoid cardamonin has the potential to interact with the TIME and exert its action by modulating different pathways. The data show that cardamonin significantly decreased MUC1 and STAT3 expression in the stimulated MDA-231 and MDA-468 cells and downregulated JAK1 mRNA expression only in MD-231 cells. It also demonstrates that cardamonin significantly increased the Nrf2 protein expression in both stimulated TNBC cell lines. In MDA-231 cells, there was a 74% inhibition on the mRNA expression of PD-L1, and in MDA-468 cells, there was an inhibition of 84%, showing a higher decrease of PD-L1 levels in the MDA-468 cells. Cardamonin also decreased PD-L1 protein expression, confirming the data on the transcription level in both stimulated TNBC cell lines. In MDA-231 cells, at the highest concentration of cardamonin (50 μM), the protein expression of PD-L1 was inhibited by 59%, and in MDA-468 cells, the inhibition of PD-L1 protein expression reached 100%. When cardamonin and TNF-α were combined, there was a 3 and 5-fold decrease in CCL2 protein expression in the MDA-231 and MDA-468 cells, respectively. In addition, using the STRING database, the functional enrichment analysis of proteins indicated that all the interactions surpassed the lowest confidence index, showing medium to high association, confirming a strong correlation between the genes and proteins selected in this study. Therefore, modulation of the expression of genes and proteins of the different signaling pathways examined in this investigation shows cardamonin's potent anticancer effects through remodeling of the TIME.

Conclusion

The present investigation shows that cardamonin significantly reduced the expression of PD-L1 and CCL2 in TNBC cells, suggesting that this inhibition could lead to lower levels of PD-L1 and subsequent blockage of tumor resistance that happens over time. This study also elucidated some of the cardamonin's molecular mechanisms involved in PD-L1 downregulation, targeting the JAK/STAT axis and MUC1 production. Moreover, cardamonin was effective in increasing levels of Nrf2, which is directly related to the decrease in NF-κB activation and consequent reduction in CCL2 levels (**Figure 9**). Therefore, the results obtained show potential anticancer effects of cardamonin through its potent ability to modulate the different genes and proteins of the TIME, indicating that cardamonin can be considered a promising candidate along with immune therapy for TNBC.

Acknowledgements

The research reported in this project was supported by the National Institute on Minority Health and Health Disparities of the National Institutes of Health under Award Number U54 MD007582.

Disclosure of conflict of interest

None.

Address correspondence to: Karam FA Soliman, Division of Pharmaceutical Sciences, College of Pharmacy and Pharmaceutical Sciences, Institute of

Public Health, Florida A&M University, Tallahassee, FL 32307, The United States. Tel: 1-850-599-3306; E-mail: karam.soliman@famu.edu

References

[1] Keenan T, Moy B, Mroz EA, Ross K, Niemierko A, Rocco JW, Isakoff S, Ellisen LW and Bardia A. Comparison of the genomic landscape between primary breast cancer in African American versus white women and the association of racial differences with tumor recurrence. J Clin Oncol 2015; 33: 3621-3627.

[2] Marra A, Trapani D, Viale G, Criscitiello C and Curigliano G. Practical classification of triple-negative breast cancer: intratumoral heterogeneity, mechanisms of drug resistance, and novel therapies. NPJ Breast Cancer 2020; 6: 54.

[3] Kinnel B, Singh SK, Oprea-Ilies G and Singh R. Targeted therapy and mechanisms of drug resistance in breast cancer. Cancers (Basel) 2023; 15: 1320.

[4] Topalian SL, Drake CG and Pardoll DM. Immune checkpoint blockade: a common denominator approach to cancer therapy. Cancer Cell 2015; 27: 450-461.

[5] Binnewies M, Roberts EW, Kersten K, Chan V, Fearon DF, Merad M, Coussens LM, Gabrilovich DI, Ostrand-Rosenberg S, Hedrick CC, Vonderheide RH, Pittet MJ, Jain RK, Zou W, Howcroft TK, Woodhouse EC, Weinberg RA and Krummel MF. Understanding the tumor immune microenvironment (TIME) for effective therapy. Nat Med 2018; 24: 541-550.

[6] Balkwill FR, Capasso M and Hagemann T. The tumor microenvironment at a glance. J Cell Sci 2012; 125: 5591-5596.

[7] Jin J, Lin J, Xu A, Lou J, Qian C, Li X, Wang Y, Yu W and Tao H. CCL2: an important mediator between tumor cells and host cells in tumor microenvironment. Front Oncol 2021; 11: 722916.

[8] Nakatsumi H, Matsumoto M and Nakayama KI. Noncanonical pathway for regulation of CCL2 expression by an mTORC1-FOXK1 axis promotes recruitment of tumor-associated macrophages. Cell Rep 2017; 21: 2471-2486.

[9] Muthuswamy R, Berk E, Junecko BF, Zeh HJ, Zureikat AH, Normolle D, Luong TM, Reinhart TA, Bartlett DL and Kalinski P. NF-κB hyperactivation in tumor tissues allows tumor-selective reprogramming of the chemokine microenvironment to enhance the recruitment of cytolytic T effector cells. Cancer Res 2012; 72: 3735-3743.

[10] Tu MM, Abdel-Hafiz HA, Jones RT, Jean A, Hoff KJ, Duex JE, Chauca-Diaz A, Costello JC, Dancik GM, Tamburini BAJ, Czerniak B, Kaye J and Theodorescu D. Inhibition of the CCL2 receptor, CCR2, enhances tumor response to immune checkpoint therapy. Commun Biol 2020; 3: 720.

[11] Maimela NR, Liu S and Zhang Y. Fates of CD8+ T cells in tumor microenvironment. Comput Struct Biotechnol J 2018; 17: 1-13.

[12] Choi J, Lee HJ, Yoon S, Ryu HM, Lee E, Jo Y, Seo S, Kim D, Lee CH, Kim W, Ha JY, Kim SY, Gong G, Jung KH, Park SR, Kim SW, Park KS and Lee DH. Blockade of CCL2 expression overcomes intrinsic PD-1/PD-L1 inhibitor-resistance in transglutaminase 2-induced PD-L1 positive triple negative breast cancer. Am J Cancer Res 2020; 10: 2878-2894.

[13] Jiang X, Wang J, Deng X, Xiong F, Ge J, Xiang B, Wu X, Ma J, Zhou M, Li X, Li Y, Li G, Xiong W, Guo C and Zeng Z. Role of the tumor microenvironment in PD-L1/PD-1-mediated tumor immune escape. Mol Cancer 2019; 18: 10.

[14] Zhu B, Tang L, Chen S, Yin C, Peng S, Li X, Liu T, Liu W, Han C, Stawski L, Xu ZX, Zhou G, Chen X, Gao X, Goding CR, Xu N, Cui R and Cao P. Targeting the upstream transcriptional activator of PD-L1 as an alternative strategy in melanoma therapy. Oncogene 2018; 37: 4941-4954.

[15] Manguso RT, Pope HW, Zimmer MD, Brown FD, Yates KB, Miller BC, Collins NB, Bi K, LaFleur MW, Juneja VR, Weiss SA, Lo J, Fisher DE, Miao D, Van Allen E, Root DE, Sharpe AH, Doench JG and Haining WN. In vivo CRISPR screening identifies Ptpn2 as a cancer immunotherapy target. Nature 2017; 547: 413-418.

[16] Pan D, Kobayashi A, Jiang P, Ferrari de Andrade L, Tay RE, Luoma AM, Tsoucas D, Qiu X, Lim K, Rao P, Long HW, Yuan GC, Doench J, Brown M, Liu XS and Wucherpfennig KW. A major chromatin regulator determines resistance of tumor cells to T cell-mediated killing. Science 2018; 359: 770-775.

[17] Paz-Ares L, Vicente D, Tafreshi A, Robinson A, Soto Parra H, Mazières J, Hermes B, Cicin I, Medgyasszay B, Rodríguez-Cid J, Okamoto I, Lee S, Ramlau R, Vladimirov V, Cheng Y, Deng X, Zhang Y, Bas T, Piperdi B and Halmos B. A randomized, placebo-controlled trial of pembrolizumab plus chemotherapy in patients with metastatic squamous NSCLC: protocol-specified final analysis of KEYNOTE-407. J Thorac Oncol 2020; 15: 1657-1669.

[18] Herbst RS, Giaccone G, de Marinis F, Reinmuth N, Vergnenegre A, Barrios CH, Morise M, Felip E, Andric Z, Geater S, Özgüroğlu M, Zou W, Sandler A, Enquist I, Komatsubara K, Deng Y, Kuriki H, Wen X, McCleland M, Mocci S, Jassem J and Spigel DR. Atezolizumab for first-line treatment of PD-L1-selected patients with NSCLC. N Engl J Med 2020; 383: 1328-1339.

[19] Rittmeyer A, Barlesi F, Waterkamp D, Park K, Ciardiello F, von Pawel J, Gadgeel SM, Hida T, Kowalski DM, Dols MC, Cortinovis DL, Leach J,

Polikoff J, Barrios C, Kabbinavar F, Frontera OA, De Marinis F, Turna H, Lee JS, Ballinger M, Kowanetz M, He P, Chen DS, Sandler A and Gandara DR; OAK Study Group. Atezolizumab versus docetaxel in patients with previously treated non-small-cell lung cancer (OAK): a phase 3, open-label, multicentre randomised controlled trial. Lancet 2017; 389: 255-265.

[20] Xue S, Cheng J, Ma W, Chen KL, Liu Y and Li J. Comparison of lipoxygenase, cyclooxygenase, xanthine oxidase inhibitory effects and cytotoxic activities of selected flavonoids. DEStech Trans Environ Energy Earth Sci 2017; 10.

[21] Feliciano RP, Pritzel S, Heiss C and Rodriguez-Mateos A. Flavonoid intake and cardiovascular disease risk. Curr Opin Food Sci 2015; 2: 92-99.

[22] Rodríguez-García C, Sánchez-Quesada C and J Gaforio J. Dietary flavonoids as cancer chemopreventive agents: an updated review of human studies. Antioxidants (Basel) 2019; 8: 137.

[23] Yahfoufi N, Alsadi N, Jambi M and Matar C. The immunomodulatory and anti-inflammatory role of polyphenols. Nutrients 2018; 10: 1618.

[24] Abotaleb M, Samuel SM, Varghese E, Varghese S, Kubatka P, Liskova A and Büsselberg D. Flavonoids in cancer and apoptosis. Cancers (Basel) 2018; 11: 28.

[25] Chirumbolo S, Bjørklund G, Lysiuk R, Vella A, Lenchyk L and Upyr T. Targeting cancer with phytochemicals via their fine tuning of the cell survival signaling pathways. Int J Mol Sci 2018; 19: 3568.

[26] Kong W, Li C, Qi Q, Shen J and Chang K. Cardamonin induces G2/M arrest and apoptosis via activation of the JNK-FOXO3a pathway in breast cancer cells. Cell Biol Int 2020; 44: 177-188.

[27] Shrivastava S, Jeengar MK, Thummuri D, Koval A, Katanaev VL, Marepally S and Naidu VGM. Cardamonin, a chalcone, inhibits human triple negative breast cancer cell invasiveness by downregulation of Wnt/β-catenin signaling cascades and reversal of epithelial-mesenchymal transition. Biofactors 2017; 43: 152-169.

[28] Niu P, Li J, Chen H, Zhu Y, Zhou J and Shi D. Anti-proliferative effect of cardamonin on mTOR inhibitor-resistant cancer cells. Mol Med Rep 2020; 21: 1399-1407.

[29] Lu S, Lin C, Cheng X, Hua H, Xiang T, Huang Y and Huang X. Cardamonin reduces chemotherapy resistance of colon cancer cells via the TSP50/NF-κB pathway in vitro. Oncol Lett 2018; 15: 9641-9646.

[30] Park S, Gwak J, Han SJ and Oh S. Cardamonin suppresses the proliferation of colon cancer cells by promoting β-catenin degradation. Biol Pharm Bull 2013; 36: 1040-1044.

[31] Wang Z, Tang X, Wu X, Yang M, Wang W, Wang L, Tang D and Wang D. Cardamonin exerts antigastric cancer activity via inhibiting LncRNA-PVT1-STAT3 axis. Biosci Rep 2019; 39: BSR20190357.

[32] Zhou X, Zhou R, Li Q, Jie X, Hong J, Zong Y, Dong X, Zhang S, Li Z and Wu G. Cardamonin inhibits the proliferation and metastasis of non-small-cell lung cancer cells by suppressing the PI3K/Akt/mTOR pathway. Anticancer Drugs 2019; 30: 241-250.

[33] He W, Jiang Y, Zhang X, Zhang Y, Ji H and Zhang N. Anticancer cardamonin analogs suppress the activation of NF-kappaB pathway in lung cancer cells. Mol Cell Biochem 2014; 389: 25-33.

[34] Niu P, Shi D, Zhang S, Zhu Y and Zhou J. Cardamonin enhances the anti-proliferative effect of cisplatin on ovarian cancer. Oncol Lett 2018; 15: 3991-3997.

[35] Zhang J, Sikka S, Siveen KS, Lee JH, Um JY, Kumar AP, Chinnathambi A, Alharbi SA, Basappa, Rangappa KS, Sethi G and Ahn KS. Cardamonin represses proliferation, invasion, and causes apoptosis through the modulation of signal transducer and activator of transcription 3 pathway in prostate cancer. Apoptosis 2017; 22: 158-168.

[36] Pascoal AC, Ehrenfried CA, Lopez BG, de Araujo TM, Pascoal VD, Gilioli R, Anhê GF, Ruiz AL, Carvalho JE, Stefanello ME and Salvador MJ. Antiproliferative activity and induction of apoptosis in PC-3 cells by the chalcone cardamonin from Campomanesia adamantium (Myrtaceae) in a bioactivity-guided study. Molecules 2014; 19: 1843-1855.

[37] STRING: functional protein association networks. 2024.

[38] Mendonca P, Alghamdi S, Messeha S and Soliman KFA. Pentagalloyl glucose inhibits TNF-α-activated CXCL1/GRO-α expression and induces apoptosis-related genes in triple-negative breast cancer cells. Sci Rep 2021; 11: 5649.

[39] Messeha SS, Zarmouh NO, Antonie L and Soliman KFA. Sanguinarine inhibition of TNF-α-induced CCL2, IKBKE/NF-κB/ERK1/2 signaling pathway, and cell migration in human triple-negative breast cancer cells. Int J Mol Sci 2022; 23: 8329.

[40] Wei F, Tang L, He Y, Wu Y, Shi L, Xiong F, Gong Z, Guo C, Li X, Liao Q, Zhang W, Ni Q, Luo J, Li X, Li Y, Peng C, Chen X, Li G, Xiong W and Zeng Z. BPIFB1 (LPLUNC1) inhibits radioresistance in nasopharyngeal carcinoma by inhibiting VTN expression. Cell Death Dis 2018; 9: 432.

[41] Quail DF and Joyce JA. Microenvironmental regulation of tumor progression and metastasis. Nat Med 2013; 19: 1423-1437.

[42] Wang JP, Tang YY, Fan CM, Guo C, Zhou YH, Li Z, Li XL, Li Y, Li GY, Xiong W, Zeng ZY and Xiong F. The role of exosomal non-coding RNAs in cancer metastasis. Oncotarget 2017; 9: 12487-12502.
[43] Li JJ, Tsang JY and Tse GM. Tumor microenvironment in breast cancer-updates on therapeutic implications and pathologic assessment. Cancers (Basel) 2021; 13: 4233.
[44] Jiang XJ, Wang J, Deng XY, Li XL, Li XY, Zeng ZY, Xiong W, Li GY, Xiong F and Guo C. Immunotherapy targeted to immune checkpoint: a revolutionary breakthrough in cancer therapy. Prog Biochem Biophys 2018; 45: 1178-1186.
[45] Tie Y, Tang F, Wei YQ and Wei XW. Immunosuppressive cells in cancer: mechanisms and potential therapeutic targets. J Hematol Oncol 2022; 15: 61.
[46] Pardoll DM. The blockade of immune checkpoints in cancer immunotherapy. Nat Rev Cancer 2012; 12: 252-264.
[47] Tsang JY, Au WL, Lo KY, Ni YB, Hlaing T, Hu J, Chan SK, Chan KF, Cheung SY and Tse GM. PD-L1 expression and tumor infiltrating PD-1+ lymphocytes associated with outcome in HER2+ breast cancer patients. Breast Cancer Res Treat 2017; 162: 19-30.
[48] Muenst S, Soysal SD, Gao F, Obermann EC, Oertli D and Gillanders WE. The presence of programmed death 1 (PD-1)-positive tumor-infiltrating lymphocytes is associated with poor prognosis in human breast cancer. Breast Cancer Res Treat 2013; 139: 667-676.
[49] Bertucci F and Gonçalves A. Immunotherapy in breast cancer: the emerging role of PD-1 and PD-L1. Curr Oncol Rep 2017; 19: 64.
[50] Beckers RK, Selinger CI, Vilain R, Madore J, Wilmott JS, Harvey K, Holliday A, Cooper CL, Robbins E, Gillett D, Kennedy CW, Gluch L, Carmalt H, Mak C, Warrier S, Gee HE, Chan C, McLean A, Walker E, McNeil CM, Beith JM, Swarbrick A, Scolyer RA and O'Toole SA. Programmed death ligand 1 expression in triple-negative breast cancer is associated with tumour-infiltrating lymphocytes and improved outcome. Histopathology 2016; 69: 25-34.
[51] Mittendorf EA, Philips AV, Meric-Bernstam F, Qiao N, Wu Y, Harrington S, Su X, Wang Y, Gonzalez-Angulo AM, Akcakanat A, Chawla A, Curran M, Hwu P, Sharma P, Litton JK, Molldrem JJ and Alatrash G. PD-L1 expression in triple-negative breast cancer. Cancer Immunol Res 2014; 2: 361-370.
[52] Ai L, Chen J, Yan H, He Q, Luo P, Xu Z and Yang X. Research status and outlook of PD-1/PD-L1 inhibitors for cancer therapy. Drug Des Devel Ther 2020; 14: 3625-3649.
[53] Bagchi S, Yuan R and Engleman EG. Immune checkpoint inhibitors for the treatment of cancer: clinical impact and mechanisms of response and resistance. Annu Rev Pathol 2021; 16: 223-249.
[54] Mimura K, Teh JL, Okayama H, Shiraishi K, Kua LF, Koh V, Smoot DT, Ashktorab H, Oike T, Suzuki Y, Fazreen Z, Asuncion BR, Shabbir A, Yong WP, So J, Soong R and Kono K. PD-L1 expression is mainly regulated by interferon gamma associated with JAK-STAT pathway in gastric cancer. Cancer Sci 2018; 109: 43-53.
[55] Bellucci R, Martin A, Bommarito D, Wang K, Hansen SH, Freeman GJ and Ritz J. Interferon-γ-induced activation of JAK1 and JAK2 suppresses tumor cell susceptibility to NK cells through upregulation of PD-L1 expression. Oncoimmunology 2015; 4: e1008824.
[56] Imai D, Yoshizumi T, Okano S, Itoh S, Ikegami T, Harada N, Aishima S, Oda Y and Maehara Y. IFN-γ promotes epithelial-mesenchymal transition and the expression of PD-L1 in pancreatic cancer. J Surg Res 2019; 240: 115-123.
[57] Sudoyo AW, Kurniawan AN, Kusumo GD, Putra TP, Rexana FA, Yunus M, Budiyati AD, Kurniawan D, Utama A and Utomo AR. Increased CD8 tumor infiltrating lymphocytes in colorectal cancer microenvironment supports an adaptive immune resistance mechanism of PD-L1 expression. Asian Pac J Cancer Prev 2019; 20: 3421-3427.
[58] Meyer SC. Mechanisms of resistance to JAK2 inhibitors in myeloproliferative neoplasms. Hematol Oncol Clin North Am 2017; 31: 627-642.
[59] Gotthardt D, Putz EM, Grundschober E, Prchal-Murphy M, Straka E, Kudweis P, Heller G, Bago-Horvath Z, Witalisz-Siepracka A, Cumaraswamy AA, Gunning PT, Strobl B, Müller M, Moriggl R, Stockmann C and Sexl V. STAT5 is a key regulator in NK cells and acts as a molecular switch from tumor surveillance to tumor promotion. Cancer Discov 2016; 6: 414-429.
[60] Kufe DW. MUC1-C oncoprotein as a target in breast cancer: activation of signaling pathways and therapeutic approaches. Oncogene 2013; 32: 1073-1081.
[61] Raina D, Agarwal P, Lee J, Bharti A, McKnight CJ, Sharma P, Kharbanda S and Kufe D. Characterization of the MUC1-C cytoplasmic domain as a cancer target. PLoS One 2015; 10: e0135156.
[62] Alam M, Ahmad R, Rajabi H, Kharbanda A and Kufe D. MUC1-C oncoprotein activates ERK→C/EBPβ signaling and induction of aldehyde dehydrogenase 1A1 in breast cancer cells. J Biol Chem 2013; 288: 30892-30903.
[63] Raina D, Uchida Y, Kharbanda A, Rajabi H, Panchamoorthy G, Jin C, Kharbanda S, Scaltriti M, Baselga J and Kufe D. Targeting the MUC1-C oncoprotein downregulates HER2 activation and abrogates trastuzumab resistance in

breast cancer cells. Oncogene 2014; 33: 3422-3431.
[64] Ahmad R, Raina D, Joshi MD, Kawano T, Ren J, Kharbanda S and Kufe D. MUC1-C oncoprotein functions as a direct activator of the nuclear factor-kappaB p65 transcription factor. Cancer Res 2009; 69: 7013-7021.
[65] Agata N, Ahmad R, Kawano T, Raina D, Kharbanda S and Kufe D. MUC1 oncoprotein blocks death receptor-mediated apoptosis by inhibiting recruitment of caspase-8. Cancer Res 2008; 68: 6136-6144.
[66] David JM, Hamilton DH and Palena C. MUC1 upregulation promotes immune resistance in tumor cells undergoing brachyury-mediated epithelial-mesenchymal transition. Oncoimmunology 2016; 5: e1117738.
[67] Maeda T, Hiraki M, Jin C, Rajabi H, Tagde A, Alam M, Bouillez A, Hu X, Suzuki Y, Miyo M, Hata T, Hinohara K and Kufe D. MUC1-C induces PD-L1 and immune evasion in triple-negative breast cancer. Cancer Res 2018; 78: 205-215.
[68] Wang W, Nag SA and Zhang R. Targeting the NFκB signaling pathways for breast cancer prevention and therapy. Curr Med Chem 2015; 22: 264-289.
[69] Cogswell PC, Guttridge DC, Funkhouser WK and Baldwin AS Jr. Selective activation of NF-kappa B subunits in human breast cancer: potential roles for NF-kappa B2/p52 and for Bcl-3. Oncogene 2000; 19: 1123-1131.
[70] Yoshimura T, Li C, Wang Y and Matsukawa A. The chemokine monocyte chemoattractant protein-1/CCL2 is a promoter of breast cancer metastasis. Cell Mol Immunol 2023; 20: 714-738.
[71] Kumar S, Chatterjee M, Ghosh P, Ganguly KK, Basu M and Ghosh MK. Targeting PD-1/PD-L1 in cancer immunotherapy: an effective strategy for treatment of triple-negative breast cancer (TNBC) patients. Genes Dis 2022; 10: 1318-1350.
[72] Low-Marchelli JM, Ardi VC, Vizcarra EA, van Rooijen N, Quigley JP and Yang J. Twist1 induces CCL2 and recruits macrophages to promote angiogenesis. Cancer Res 2013; 73: 662-671.
[73] Peranzoni E, Lemoine J, Vimeux L, Feuillet V, Barrin S, Kantari-Mimoun C, Bercovici N, Guérin M, Biton J, Ouakrim H, Régnier F, Lupo A, Alifano M, Damotte D and Donnadieu E. Macrophages impede CD8 T cells from reaching tumor cells and limit the efficacy of anti-PD-1 treatment. Proc Natl Acad Sci U S A 2018; 115: E4041-E4050.
[74] Lippitz BE. Cytokine patterns in patients with cancer: a systematic review. Lancet Oncol 2013; 14: e218-228.
[75] Mariathasan S, Turley SJ, Nickles D, Castiglioni A, Yuen K, Wang Y, Kadel EE III, Koeppen H, Astarita JL, Cubas R, Jhunjhunwala S, Banchereau R, Yang Y, Guan Y, Chalouni C, Ziai J, Şenbabaoğlu Y, Santoro S, Sheinson D, Hung J, Giltnane JM, Pierce AA, Mesh K, Lianoglou S, Riegler J, Carano RAD, Eriksson P, Höglund M, Somarriba L, Halligan DL, van der Heijden MS, Loriot Y, Rosenberg JE, Fong L, Mellman I, Chen DS, Green M, Derleth C, Fine GD, Hegde PS, Bourgon R and Powles T. TGFβ attenuates tumour response to PD-L1 blockade by contributing to exclusion of T cells. Nature 2018; 554: 544-548.
[76] Peng D, Kryczek I, Nagarsheth N, Zhao L, Wei S, Wang W, Sun Y, Zhao E, Vatan L, Szeliga W, Kotarski J, Tarkowski R, Dou Y, Cho K, Hensley-Alford S, Munkarah A, Liu R and Zou W. Epigenetic silencing of TH1-type chemokines shapes tumour immunity and immunotherapy. Nature 2015; 527: 249-253.
[77] Thimmulappa RK, Scollick C, Traore K, Yates M, Trush MA, Liby KT, Sporn MB, Yamamoto M, Kensler TW and Biswal S. Nrf2-dependent protection from LPS induced inflammatory response and mortality by CDDO-Imidazolide. Biochem Biophys Res Commun 2006; 351: 883-889.
[78] Chen XL, Dodd G, Thomas S, Zhang X, Wasserman MA, Rovin BH and Kunsch C. Activation of Nrf2/ARE pathway protects endothelial cells from oxidant injury and inhibits inflammatory gene expression. Am J Physiol Heart Circ Physiol 2006; 290: H1862-1870.
[79] Levonen AL, Inkala M, Heikura T, Jauhiainen S, Jyrkkänen HK, Kansanen E, Määttä K, Romppanen E, Turunen P, Rutanen J and Ylä-Herttuala S. Nrf2 gene transfer induces antioxidant enzymes and suppresses smooth muscle cell growth in vitro and reduces oxidative stress in rabbit aorta in vivo. Arterioscler Thromb Vasc Biol 2007; 27: 741-747.
[80] Pae HO, Oh GS, Lee BS, Rim JS, Kim YM and Chung HT. 3-Hydroxyanthranilic acid, one of L-tryptophan metabolites, inhibits monocyte chemoattractant protein-1 secretion and vascular cell adhesion molecule-1 expression via heme oxygenase-1 induction in human umbilical vein endothelial cells. Atherosclerosis 2006; 187: 274-284.
[81] Satoh H, Moriguchi T, Takai J, Ebina M and Yamamoto M. Nrf2 prevents initiation but accelerates progression through the Kras signaling pathway during lung carcinogenesis. Cancer Res 2013; 73: 4158-4168.
[82] Tao S, Rojo de la Vega M, Chapman E, Ooi A and Zhang DD. The effects of NRF2 modulation on the initiation and progression of chemi-

cally and genetically induced lung cancer. Mol Carcinog 2018; 57: 182-192.
[83] DeNicola GM, Karreth FA, Humpton TJ, Gopinathan A, Wei C, Frese K, Mangal D, Yu KH, Yeo CJ, Calhoun ES, Scrimieri F, Winter JM, Hruban RH, Iacobuzio-Donahue C, Kern SE, Blair IA and Tuveson DA. Oncogene-induced Nrf2 transcription promotes ROS detoxification and tumorigenesis. Nature 2011; 475: 106-109.
[84] Wang H, Liu X, Long M, Huang Y, Zhang L, Zhang R, Zheng Y, Liao X, Wang Y, Liao Q, Li W, Tang Z, Tong Q, Wang X, Fang F, Rojo de la Vega M, Ouyang Q, Zhang DD, Yu S and Zheng H. NRF2 activation by antioxidant antidiabetic agents accelerates tumor metastasis. Sci Transl Med 2016; 8: 334ra351.
[85] Padmanabhan B, Tong KI, Ohta T, Nakamura Y, Scharlock M, Ohtsuji M, Kang MI, Kobayashi A, Yokoyama S and Yamamoto M. Structural basis for defects of Keap1 activity provoked by its point mutations in lung cancer. Mol Cell 2006; 21: 689-700.
[86] Singh A, Misra V, Thimmulappa RK, Lee H, Ames S, Hoque MO, Herman JG, Baylin SB, Sidransky D, Gabrielson E, Brock MV and Biswal S. Dysfunctional KEAP1-NRF2 interaction in non-small-cell lung cancer. PLoS Med 2006; 3: e420.
[87] Hanahan D and Weinberg RA. The hallmarks of cancer. Cell 2000; 100: 57-70.
[88] Hanahan D and Weinberg RA. Hallmarks of cancer: the next generation. Cell 2011; 144: 646-674.
[89] Menegon S, Columbano A and Giordano S. The dual roles of NRF2 in cancer. Trends Mol Med 2016; 22: 578-593.
[90] Xiang M, Namani A, Wu S and Wang X. Nrf2: bane or blessing in cancer? J Cancer Res Clin Oncol 2014; 140: 1251-1259.
[91] Sporn MB and Liby KT. NRF2 and cancer: the good, the bad and the importance of context. Nat Rev Cancer 2012; 12: 564-571.
[92] Bellezza I, Mierla AL and Minelli A. Nrf2 and NF-κB and their concerted modulation in cancer pathogenesis and progression. Cancers (Basel) 2010; 2: 483-497.
[93] Ahmed SM, Luo L, Namani A, Wang XJ and Tang X. Nrf2 signaling pathway: pivotal roles in inflammation. Biochim Biophys Acta Mol Basis Dis 2017; 1863: 585-597.